

# Journal of Engineering and Engineering Technology

ISSN 1598-0271



School of Engineering and Engineering Technology,  
The Federal University of Technology, Akure, Nigeria





## Conceptual Design of Battery Powered Vehicle for Children Amusement Park Using Nigerian Anthropometric Parameters

Ayodeji S. P., Adeyeri M. K. and Oni O. O.

Department of Mechanical Engineering, The Federal University of Technology, Akure, Nigeria.

### A B S T R A C T

#### Key words:

Conceptual Design, Battery Powered Vehicle, Children, Amusement Park, Anthropometric Parameters

*Exercise helps children to be active and lack of it can lead to boredom. The problem of unavailability of facilities designed for children amusement park using the right anthropometric parameters and the procurement cost due to importation duties have been a big challenge. Provision of children vehicle for amusement park using anthropometric parameters will go a long way to solve the problems associated with boredom. Anthropometric parameters from 250 (150 male and 100 female) children between ages 3 to 12 were collected and analysed. The 5th, 25th, 50th, 75th and 95th percentiles for female and male respectively were used in the design of the children vehicle. Detailed drawings and simulation of the design concept were produced on Autodesk Inventor CAD software. Three deep cycle battery of 200Ah x 12V each was proposed as the energy driver that will drive the vehicle for 1hr at a carrying load capacity of 2280N. The simulation result ensure the stability of the vehicle*

### 1. Introduction

Playing is important to children's healthy development and learning. Almost everything that a growing child needs to learn is developed, acquired and practiced while playing. Most of what children learnt include concrete skills, such as counting, motor co-ordination, speech and abstract skills, including imagination, problem-solving, planning and learning. Children vehicle is an important facility that makes children happy at amusement park (De Groot, 2009). Availability of such facility that makes children engage in constructive play will reduce the effect of boredom on children which make them to misbehave.

In Nigeria, there are some reports on design using anthropometric parameters which are mainly for adults, youths and the physically challenged (Ayodeji et al., 2015; Ayodeji and Adeyeri, 2011; Ismaila et al., 2010). Ayodeji et al. (2015) design an adaptive left throttling pedal vehicle for paraplegic, the design however found application to the physically challenged. Ayodeji and Adeyeri (2011) designed a tricycle which can easily be produced locally for paraplegic, this as well applies to the physically challenged. Ismaila et al (2010) did an anthropometric survey and appraisal of furniture

for Nigerian primary school pupils, they also concluded that the chairs and desks use by Nigerian primary school pupils were probably design using British anthropometric data or none at all is design using the users anthropometric data because some of the dimensions were high while others were low for the pupil. There has been no report that show detailed anthropometric parameter that can be used in design of children vehicle for Nigerian population. There are some reports on the design of battery powered amusement vehicle for Children outside Nigeria like Beneito et al. (2007) who designed and developed of an electric toy vehicle powered by a fuel cell stack which uses hydrogen as the source of energy. All the vehicles in Nigerian amusement park are imported which are designed using the anthropometric parameter of the country in which they were produced.

This research work is focused on producing conceptual design of children amusement battery powered vehicle using the anthropometric parameters of Nigerian children and locally available resources.

### 2.0 Materials and Methods

Children anthropometric parameters were collected in primary schools using the following anthropometer: weighing machine/scale for weight measurement, flexible tape rule for

Correspondence:

E-mail address: ayodejisesantut@gmail.com, [adeyerimichaeltut@gmail.com](mailto:adeyerimichaeltut@gmail.com)

+2348036709782, +2348060218116, +2347033714943

circular part and wooden sliding caliper for horizontal measurement. The data collected were analysed to determine the 5th, 25th, 50th, 75th and 95th percentile which were used in the design of the vehicle.

The detailed drawing of the vehicle was produced with Autodesk Inventor CAD software and analysis of each component part was done using appropriate equations.

In the design of the vehicle the following factors were considered to improve the efficiency of the vehicle; the weight of the vehicle, ease of fabrication, ergonomics (the comfort of the users), the material for each component part was considered base on their availability, Physical and mechanical properties of the material, reliability of the material, Maintainability and Cost-effectiveness.

Animation and simulation of the design vehicle were carried out using Autodesk inventor CAD software to ensure functionality of the vehicle before production performance evaluation will be carried out to determine the following: maximum speed; stability; power consumption and safety of use by children after fabrication.

### 2.1 Design Analysis of Component Parts of the Children Vehicle

The major components of the proposed vehicle are; the steering system, the suspension system, the electric motor, battery, the chassis and frame, the tires and wheels, the door and the seat.

#### 2.1.1 Power Required Determination

In order to determine the power required to propel the children vehicle, the resistance force needs to be calculated. According to Young et al., (2013) and Kim et al., (2013), the resistive forces are the sum of the rolling resistance between tires and road surface, aerodynamic drag, and uphill grading resistance as shown in equation (1)

$$F_w = F_r + F_l + F_{gr} + F_a \quad (1)$$

Where  $F_w$  is total resistive force,  $F_r$  is rolling resistance,  $F_l$  is Aerodynamic resistance,  $F_{gr}$  is Graded resistance and  $F_a$  is Acceleration resistance

#### 2.1.2 Rolling Resistance:

is the opposing force that the vehicle has to overcome due to the rolling motion between the wheels and the surface of motion of the vehicle. The rolling resistance was determined using equation (2). The rolling resistance depends on the co-efficient of rolling friction which varies depending upon the material of tyres and the roughness of the surface of motion (Dorobantu, 2013).

$$F_r = fm + Mg \quad (2)$$

Where  $fm$  is coefficient of rolling resistance,  $M$  is the mass of the vehicle and the users,  $g$  is acceleration due to gravity. The mass of

the vehicle according to the result from Autodesk Inventor is 152kg and the mass of a child from 95th percentile of mass of children measured is 38kg. The total weight of the vehicle and two children is 228Kg. The children vehicle will be driven on tile, field, cement mat or carpet.

An exact value for the coefficient of rolling resistance for these surfaces was unavailable; therefore, coefficient of rolling resistance for an unpaved road was used. The value will be greater than that of the carpet and ensures that the vehicle will be capable of being driven on very rough surfaces. According to Mukherjee (2014) the coefficient of rolling resistance for an unpaved surface is 0.05. Using equation (2) the rolling force is determined to be 111.72N

Gradient resistance is an important factor in total resistive resistance. The vehicle is expected to be able to ascend on a sloppy surface. Graded resistance was calculated using equation (3) to be 578.31

$$F_{gr} = Mg \sin \alpha \quad (3)$$

Where  $\alpha$  is the gradient angle which is  $15^\circ$ .

Thus acceleration resistance was determined using equation (4)

Acceleration force is the force that helps the vehicle to reach a predefined speed from rest in a specified period of time. The motor torque bears a direct relationship with the acceleration force. Better the torque, lesser the time required by the vehicle to reach a given speed. The acceleration force is a function of the mass of the vehicle (Young et al., 2013). To calculate acceleration resistance ( $F_a$ ), the actual acceleration required was determined using equation (4). The vehicle is required to travel with a maximum velocity of  $4\text{ms}^{-1}$

$$a = \frac{v-u}{t} \quad (4)$$

$u$  is the Initial speed which is zero,  $v$  is the highest expected velocity,  $t$  is the Rise time which is 1s Therefore acceleration is  $4\text{ms}^{-2}$  and thus acceleration resistance was determined to be 912N using equation (5)

$$F_a = Ma$$

#### 2.1.3 Aerodynamics Resistance ( $F_l$ )

This is the resistance force caused by air drag. It was assumed to be negligible due to the relatively low speed of the vehicle

The total resistance force was calculated to be 1602.03N using equation 1

According to Kim et al. (2013), the power required to propel the vehicle is the product of sum of resistance force ( $F_w$ ) and the speed of the car ( $v$ ) as shown in equation (6) and was determined to be 6.4kW

$$\text{Power}(P) = F_w \times V$$

The value of the power was used to determine the type of battery

## 2.6 Steering Design

Ackerman steering geometry principle was adopted in the design of the vehicle steering system. The principle state that during turning if the centers of all wheels meet at a point, then the vehicle will take turn about that point which results in pure rolling of the vehicle (Koladia, 2014). The condition is called the Ackerman condition and this principle is known as Ackerman principle as shown in Fig. 2. According to Mitchell et al (2006) Jeanfoud principle establish that for the turn center of all the wheel to be the same, the extension of the steering arm must join with the center of the rear axle as show in Fig. 3

Ackerman condition for two wheels steering is expressed as in equation (8) according to Koladia (2014):

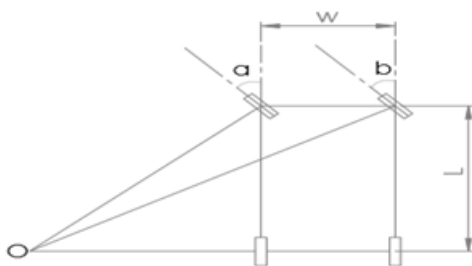


Fig. 2: Ackerman Steering Geometry

$$\cot\delta_o - \cot\delta_i = \frac{w}{L} \quad (8)$$

Where,  $\delta_o$  is the outer wheel angle,  $\delta_i$  is the inner wheel angle,  $w$  is the distance between left and right kingpin centerline and  $L$  is the wheel base of the vehicle. Equation (8) was used to calculate the value of the angle (b) for any value of the angle (a).

## 3.0 Result and Discussion

The result of the anthropometric data collected was analysed to determine the mean, 5th, 25th, 50th, 75th and 90th percentile for both male and female as shown in Table 1 and 2 respectively. The data was used in the design of the vehicle. Figure 4 show the exterior part of the vehicle while Figure 5 and 6 show the interior part and the exploded view respectively.

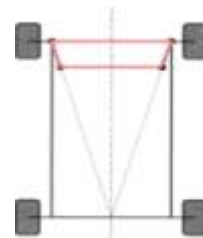


Fig. 3: Jeanfoud Trapezium

Table 2: Male Anthropometric parameters

Category	Mean	percentile				
		5 <sup>th</sup>	25 <sup>th</sup>	50 <sup>th</sup>	75 <sup>th</sup>	95 <sup>th</sup>
<b>Age (yrs)</b>	7.89	3.00	5.00	8.00	11.00	12.00
<b>Weight (kg)</b>	26.41	14.00	20.00	28.50	32.00	35.95
<b>Full height (cm)</b>	123.93	92.05	108.50	127.00	138.80	153.1
<b>Sitting height (cm)</b>	62.55	53.50	58.00	63.00	68.00	69.10
<b>Forward Reach (cm)</b>	58.26	38.53	49.98	58.80	66.30	71.90
<b>Eye height(sitting) (cm)</b>	51.37	40.03	46.03	52.10	55.63	66.00
<b>Mid Shoulder Height (cm)</b>	39.62	32.14	35.23	40.05	43.70	46.76
<b>Buttock to keel length (cm)</b>	42.21	31.10	36.00	43.25	48.00	52.90
<b>Popliteal Height (sitting) (cm)</b>	32.77	23.00	28.85	33.60	36.45	38.99
<b>Elbow to Finger Tip length (cm)</b>	35.20	26.50	31.65	35.20	38.30	43.00
<b>Waist Depth (cm)</b>	17.69	14.80	16.23	17.55	19.00	21.77
<b>Buttock to Heel Length (cm)</b>	72.27	50.50	63.65	73.90	81.18	89.90
<b>Shoulder Breadth (cm)</b>	31.08	24.60	28.50	32.00	33.00	35.00
<b>Hip Breadth (cm)</b>	22.97	17.22	19.00	23.20	25.28	29.00
<b>Forearm to Forearm Breadth (cm)</b>	31.08	24.04	28.35	32.05	33.58	36.29
<b>Elbow Rest Height (cm)</b>	13.18	9.50	10.50	12.70	15.65	18.20

and electric motor that was used for the vehicle.

2.1.4 Torque

The amount of torque required at the wheels of the vehicle was found to be 961.2 Nm using equation (7)

$$\tau = F_w r \tag{7}$$

Where r is the wheel radius which is equal to 0.15m.

The choice of battery and electric motor was made based on the calculated power and torque respectively

2.2 The Circuit Diagram

The circuit diagram of the vehicle as shown in Fig. 1 consists of major components such as the Battery, Motor controller, Contactor, Electric motor fuse, switch and other components.

Power is transmitted to the motor controller from the deep cycle batteries connected in series to the electric motor, the speed and its speed. The torque of the electric motor is regulated by controller. Other electrical unit such as ignition button, lightning, Horn are powered via a step down transformer. The electrical system is protected by the contactor to prevent overloading and surge.

2.3 Battery

Deep cycle lead ion batteries was used in powering the vehicle because of its ability to provide a steady amount of current over a long period of time compared to a lead acid batteries. It allows deeper discharges and use 80 percent of its charges

2.3.1 Determination of Battery Specification

The vehicle battery is designed to use a high capacity 200Ah x 12V batteries because of its compatibility and space conservation. The battery was connected in series, as series connection is used when a longer discharge time is required.

The power requirement of the vehicle as calculated in equation 6 is 6.4kW

A single battery is expected to generate (200Ah x 12V) = 2.4kW/hr

These batteries are connected in series to achieve a longer period in operation, when the batteries are connected in series, three batteries are expected to generate, 200Ah x 36V = 7.200kW/hr

The connected batteries must be the same capacity, age and type to avoid voltage imbalance.

2.4 Recharge time:

The three batteries are expected to drive the vehicle for at least one hour before is being recharged since the power requirement of the vehicle is 6.4 kW and the battery used will produce 7.2kW/hr.

2.5 The Vehicle Seat:

The seat is an important part of the vehicle which was design using the collected anthropometric data in order to ensure that the seat fit the users. The percentile of the anthropometric data used in the design of the seat was adopted from Ismaila el ta (2015) is shown in Table 1

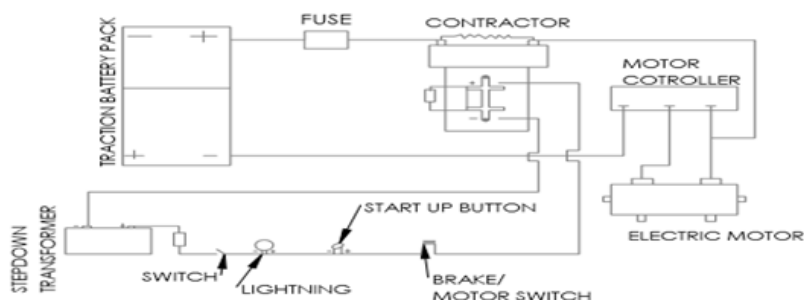


Fig 1: The Circuit Diagram

Table 1: The Anthropometric Data Used in Seat Design

Anthropometry Parameters	Percentile Used for Design	Corresponding Seat Dimension
Buttock to Popliteal	75 <sup>th</sup> Percentile Male	Seat Length
Hip Breadth (Seating)	95 <sup>th</sup> Percentile Female	Seat Width
Mid- Shoulder Height	75 <sup>th</sup> Percentile Male	Seat to Top of Backrest
Maximum Body Width	95 <sup>th</sup> Percentile Female	Backrest Width
Popliteal Height (Sitting)	75 <sup>th</sup> Percentile Female	Seat to Floor
Elbow rest height (Sitting)	5 <sup>th</sup> Percentile	Elbow Rest Height

Source: Ismaila el ta., 2015

Table 3: Female Anthropometric Parameters

Category	Mean	percentile				
		5 <sup>th</sup>	25 <sup>th</sup>	50 <sup>th</sup>	75 <sup>th</sup>	95 <sup>th</sup>
Age (yrs)	7.29	3.00	5.00	7.00	10.00	12.00
Weight (kg)	24.95	14.00	19.00	24.50	30.00	38.00
Full height (cm)	118.88	88.10	103.80	124.00	133.50	151.9
Sitting height (cm)	60.82	52.02	56.63	61.00	65.88	68.98
Forward Reach (cm)	56.07	38.53	48.35	57.90	64.68	69.19
Eye height(sitting) (cm)	49.31	40.00	45.13	49.60	53.10	60.04
Mid Shoulder Height (cm)	38.70	32.00	35.00	38.20	42.20	45.78
Buttock to keel length (cm)	39.39	25.42	34.03	40.00	46.50	49.19
Popliteal Height (sitting) (cm)	31.66	22.14	28.00	32.95	36.10	38.00
Elbow to Finger Tip length (cm)	34.57	26.11	30.65	35.00	37.60	40.57
Waist Depth (cm)	17.19	14.80	15.90	17.10	18.15	20.10
Buttock to Heel Length(cm)	70.66	53.53	62.45	72.15	79.15	85.98
Shoulder Breadth(cm)	30.69	24.51	28.10	31.45	33.00	34.95
Hip Breadth (cm)	22.35	17.20	19.13	23.05	24.70	27.66
Forearm to Forearm Breadth (cm)	30.89	24.81	28.43	32.00	33.10	36.00
Elbow Rest Height	12.61	9.21	10.33	12.00	14.68	17.96

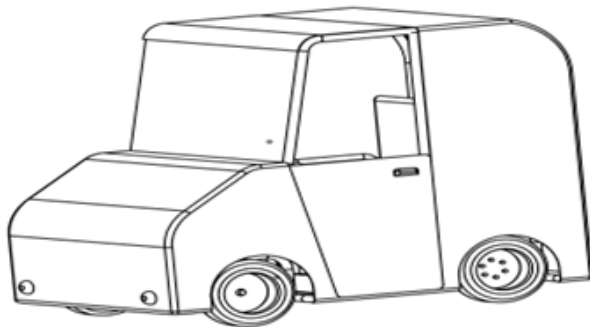


Fig. 4: The Designed Vehicle

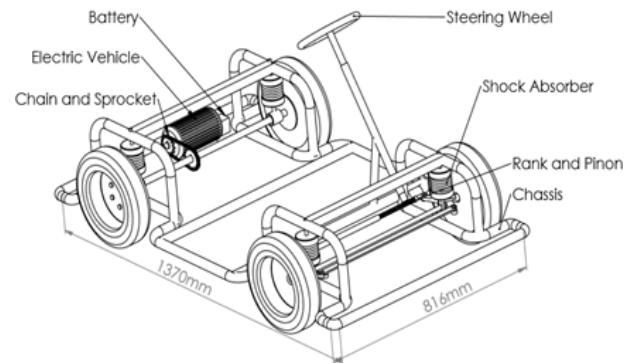


Fig 5: The Chassis, steering system and the suspension system of the Children Vehicle

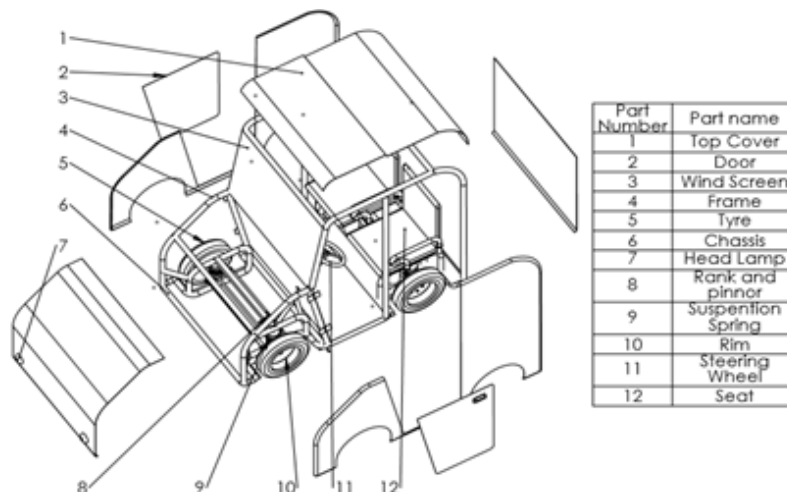


Fig 6: Exploded View of the Vehicle

A linear stress analysis was conducted on the vehicle chassis using finite element method on Autodesk inventor CAD software. This helped to determine if the chassis can withstand the weight of the vehicle under normal working condition and to check if the design can be modified to increase the factor of safety. Load of 2234.4 N which is the total weight of the Vehicle was distributed uniformly on the chassis as shown in Figure 7 which is the von Mises stress result. The red portions on the chassis show where stresses are maximal, while the portions with blue colour show where the stresses are minimal. The result show that the highest stress is 136.8 which is lower than 207 MPa, the yield stress of mild steel which is the material used in the design. The minimum factor of safety as shown in Figure 8 is 1.51 which shows that the design is save as the value is more than 1.

$$\tan \delta_o - \tan \delta_i = \frac{w}{L} \quad (8)$$

Where,  $\delta_o$  is the outer wheel angle,  $\delta_i$  is the inner wheel angle, w is

the distance between left and right kingpin centerline and L is the wheel base of the vehicle. Equation (8) was used to calculate the value of the angle (b) for any value of the angle (a).

### 3.0 Result and Discussion

The result of the anthropometric data collected was analysed to determine the mean, 5th, 25th, 50th, 75th and 90th percentile for both male and female as shown in Table 1 and 2 respectively. The data was used in the design of the vehicle. Figure 4 show the exterior part of the vehicle while Figure 5 and 6 show the interior part and the exploded view respectively.

#### Result of simulation of the suspensions system at difference speed

The result of the dynamic simulation of the vehicle that was carried out at different speed and different loading condition, were shown in Fig 9 to 15. The results revealed the behavior of the suspension system at different speeds with and without passengers.

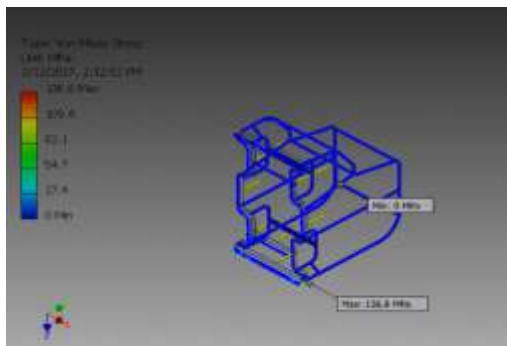


Fig 7: Von Mises Stress of forces Acting Normally on the Chassis of the Vehicle

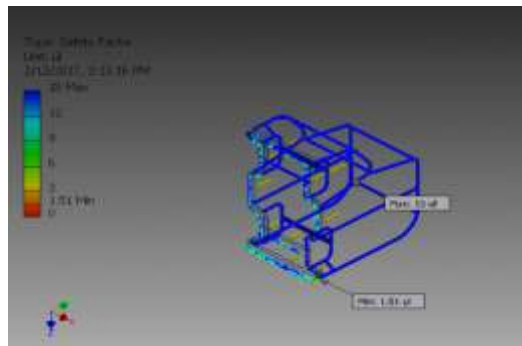


Fig. 8: Factor of safety of the forces Acting Normally on the Chassis of the Vehicle

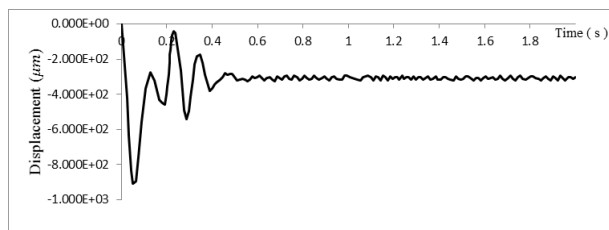


Fig 9: Graph of displacement against time for the Front suspension system when the vehicle move without passenger with a speed of 2 m/s

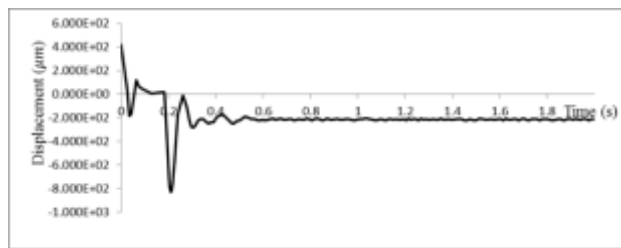


Fig 10: Graph of displacement against time for the Front suspension system when the vehicle move without passenger with a speed of 2 m/s

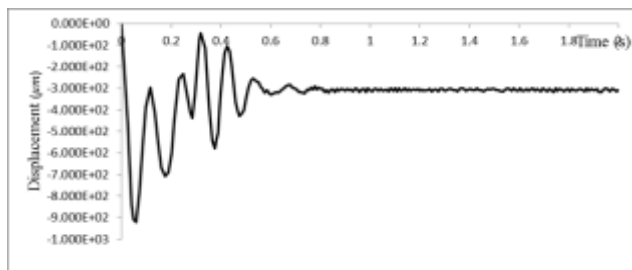


Fig 11: Graph of displacement against time for the Front suspension system when the vehicle carried a child that weighs 38 kg with a speed of 3 m/s

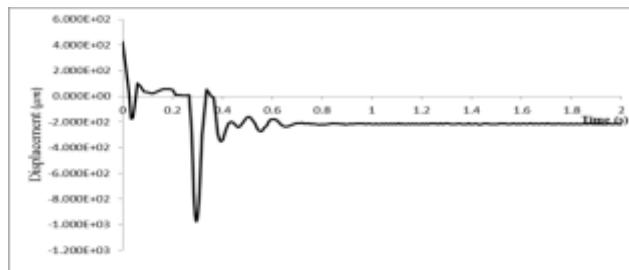


Fig 12: Graph of displacement against time for the rear suspension system when the vehicle carried a child that weighs 38 kg with a speed of 3 m/s

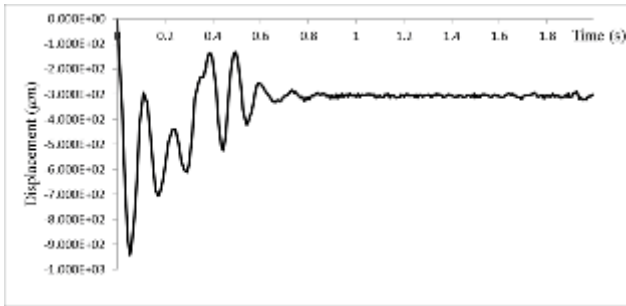


Fig 13: Graph of displacement against time for the front suspension system when the vehicle carried two children that weigh 38kg each with a speed of 4 m/s

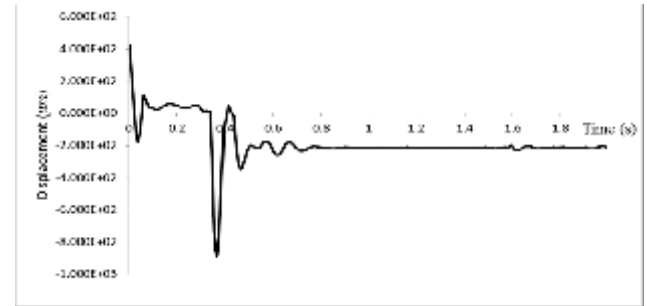


Fig 14: Graph of displacement against time for the rear suspension system when the vehicle carried two children that weigh 38kg each with a speed of 4 m/s

Fig 9 and 10 show the result obtained from a set (one out of the two at the rear and front) of spring damper system of the car simulation when the car was made to move at the speed of 2m/s with the excitation force which is the sprung weight of the vehicle. At the start, the vehicle front spring experience both transient and steady-state responses which gave the spring amplitude displacement of the range 0 to  $9 \times 10^2 \mu\text{m}$ . After 5s the transient state died off and was left with the steady state with the displacement of  $3.2 \times 10^2 \mu\text{m}$ . The rear suspension system experience similar thing as amplitude displacement covers  $19.4 \times 10^2 \mu\text{m}$ . as show in Fig 10 and the transient response died off almost at the same time with the front spring.

Fig 11 and 12 also show the result gotten from the simulation when the vehicle carried a child that weigh 38 kg and moved with a speed of 3m/s, the front spring experience a transient and steady-state response with displacement amplitude range of  $9.4 \times 10^2 \mu\text{m}$  and the transient force died off after 0.8s. The rear spring experience a transient state with displacement range of  $14 \times 10^2 \mu\text{m}$ . and the transient response also died of after 0.8s.

Fig 13 and 14 show the result gotten from the simulation when the vehicle carried two children that weigh 38 kg each and moved with a speed of 4m/s, the front spring experience a transient and steady-state response with displacement amplitude range of  $9.8 \times 10^2 \mu\text{m}$ . while the transient response died off after 0.9s. The rear spring experience a transient and steady-state response of displacement amplitude range of  $13.2 \times 10^2 \mu\text{m}$  and the transient response also died of after 0.9s.

The difference in the displacement between the front and the rear spring dampers is largely due to the load distribution of the car (center of mass) and the rear wheel moment generated by the electric motor (rear wheel drive). As show on the graphs above, both spring damper system will not return to their original state until the car is put to a stop and the imposed masses (Human) removed.

It is observed from the cases considered that the steady-state responses of the front springs are the same at a range of  $3 \times$

$10^2 \mu\text{m}$  after the transient response dies off.

The same applied to the rear springs, as they become steady at an amplitude range of  $2 \times 10^2 \mu\text{m}$ . In the 3 scenarios, the vehicle becomes relatively stable as shown from the graphs presented above after 0.8 s.

#### 4.0 Conclusion

The Nigerian children anthropometric parameter that was collected and documented in this research work was used in the design of the children battery powered vehicle for amusement park, as this will reduce user work load and the probability of accident on the users. The vehicle component parts are assembled to permit ease of disassembly, maintenance and servicing. The results of the simulation carried out show that the vehicle will work as expected if developed. The vehicle is expected to improve the standard of Nigeria amusement parks when implemented.

#### Reference

- Ayodeji, S. P. and Adeyeri, M. K. (2011): Computer Aided Assembly Animation of a Tricycle for Paraplegics. Proceedings of the World Congress on Engineering 2011 VolIII London, U.K.
- Ayodeji, S. P.; Yakubu A. M. and Fasan O. J.(2015): Design and Fabrication of an Adaptive Left Throttling Pedal for V-Boot Wagon 230 for Right LEG Paraplegic Patient. International Journal of Scientific & Engineering Research, 6:81-88.
- Beneito R, Vilaplana J, Gisbert S.(2007): Electric toy vehicle powered by a PEMFC stack. International Journal of Hydrogen Energy.32:1554–1558
- De Groote P. (2009): Globalisation of Commercial Theme Parks. Case: The Walt Disney Company. Division of Geography and tourism. ISSN 0777-2424, 38:21-28
- Dorobantu, B. (2013): Design of The Electrical Power System for A Rc-Toy Car. Journal of Industrial Design and Engineering Graphics. 8(1):13-16



- Ismaila, S. O.; Akanbi, O. G. and Oderinu, S.O. (2010). Anthropometric Survey and Appraisal of Furniture for Nigerian Primary School Pupils. e- Journal of Science & Technology, 4(5): 29-36
- Ismaila, S. O.; Akanbi, O. G.; Oderinu, S O.; Anyanwu, B. U. and Alamu, K. O.(2015): Design of Ergonomically Compliant Desks and Chairs for Primary Pupils in Ibadan, Nigeria. Journal of Engineering Science and Technology. 10: 35–46.
- Koladia, D. (2014): Mathematical Model to Design Rack And Pinion Ackerman Steering Geometry. International Journal of Scientific & Engineering Research, 5: 716-720
- Mitchell, W. C.; Staniforth A. and Scott L. (2006): Analysis of Ackermann steering system geometry, Proceedings of the 2006 Motorsports Engineering Conference and exhibition, p. 399
- [Young K.; Wang C.; Wang L. Y. and Strunz K. \(2013\): Electric Vehicle Battery Technologies. Electric Vehicle Integration into Modern Power Networks. ISBN: 978-1-4614-0133-9. Pp 15-56](#)